DEVELOPMENT AND QUALIFICATION OF INSTRUMENTED UNMANNED PLANES FOR TURBULENCE OBSERVATIONS IN THE ATMOSPHERIC SURFACE LAYER

45

ALAOUI-SOSSE, Sara[1,2]. PASTOR, Philippe[1]. DURAND, Pierre[2]. MEDINA, Patrice[2].GAVART, Michel[3].DARROZES, José[4]. LOTHON,Marie[2].

[1]ISAE-SUPAERO, Université de Toulouse, France; [2] Laboratoire d'Aérologie, Université de Toulouse, CNRS, UPS, Toulouse, France; [3] Boréal groupe MISTRAL, Castanet-Tolosan, France; [4] Univ Paul Sabatier, CNRS, GET, UMR5563,IRD,UR254, Toulouse, France.

1. Introduction

The technological advances related to the development of unmanned aircraft for atmospheric observations offer the possibility to carry out measurements in areas at very low heights that are difficult to reach by piloted aircraft, and thus to cover a wider airspace for meteorological data gathering. The drones present an opportunity to investigate the turbulence in the atmospheric surface layer in a complementary way to instrumented towers/masts. These unmanned aircraft were classified according to three main categories, depending on their weights and their payload capacities [6]. The first category regroups all UAVs weighing between 10 kg and 30 kg, like for example the Manta, ScanEagle, Aerosonde and RPMSS; their advantage is their endurance and their highest payload capacity but they are very expensive. The category II includes vehicles that weigh more than 1 kg and less than 10 kg like Tempest, the meteorological mini unmanned aerial vehicle (M2AV), University of Colorado Boulder NexSTAR, the multipurpose automatic sensor carrier (MASC), and the small multifunction autonomous research and teaching sonde (SMARTSonde). These UAVs are smaller and have less payload capacity and autonomy of flight than the vehicles of category I, nevertheless they can carry many of the sensors used for wind measurements. In addition to this, their cost is medium which makes them more easily deployable. Finally the category III, assembles UAVs that weigh less than 1 kg, for instance the small unmanned meteorological observer (SUMO) and DataHawk, which have limited payload capacity and endurance in comparison with the two other categories. Furthermore, their cost and their facility of deployment permit to do small experiences from anywhere.

Recently, we have developed in Toulouse (France) two platforms of different size. The first one, called OVLI-TA, is a small unmanned aerial system (UAS) (3kg, payload included). It is instrumented with a 5-hole probe on the nose of the airplane, a Pitot probe, a fast inertial measurement unit (IMU), a GPS receiver, as well as temperature and moisture sensors in specific housings. After wind tunnel calibrations, the drone's flight tests were conducted in Lannemezan (France), where there is an equipped 60 m tower, which constitutes a reference to our measurements. The drone then participated to the international project DACCIWA (Dynamics-Aerosol-Chemistry-Clouds Interactions In West Africa), in Benin.

Moreover, another project is carried out about the instrumentation of a so-called "Boreal" drone, which weighs 20 kg and can embark 5 kg of sensors and IMU with data fusion. The scientific payload relates to atmospheric turbulence, GNSS reflectometry and gravimetry. In addition, this UAS has a long endurance (up to 10 h) and is more robust to fly in turbulent conditions.

We will present the instrumental packages of the two UASs, the results of qualification flights of OVLI-TA as well as the first scientific results obtained in the DACCIWA campaign. We will also give some examples of envisaged deployment and observation strategy in future campaigns.

2. Technical description of our unmanned aerial systems:

2.1. Characteristics of "OVLI-TA"

The airplane utilized in the project is a Techpod, from HobbyUAV.

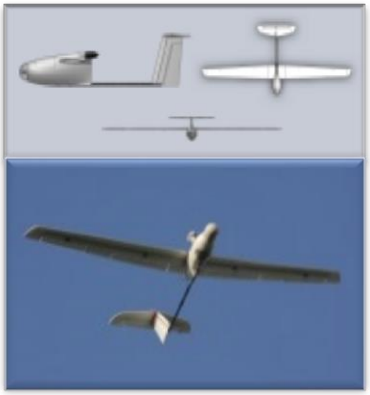

Figure 1: Pictures of OVLI-TA UAV

OVLI-TA in French stands for Objet Volant Léger Instrumenté-Turbulence Atmosphérique that means Instrumented light flying object-atmospheric turbulence. OVLI-TA is a small UAV (see Fig. 1), working with electrical propulsion. Its cruise speed is between 12 and 20m/s. It has a wingspan of 2.60 m and a fuselage length of 1.14 m. This UAV weighs 3.5 kg payload and battery included (1.25 kg without). The wings and fuselage are made from EPO (Expanded Polyolefin). It has up to two hours of autonomy.

2.2. Electronic devices on OVLI-TA :

OVLI-TA is equipped with a 100 Hz ***µ***SD card, and three temperature and humidity sensors SHT75 (2 slow sensors recorded at 2.5 Hz and 1 faster at 10 Hz) which are placed inside dedicated hoods (Fig. 2).

The ADIS16448 inertial measurement unit (IMU) includes a triaxial digital gyroscope, a triaxial digital accelerometer, a triaxial digital magnetometer, a digital barometer and an embedded temperature sensor.

One GPS and one Pitot tube were also implemented. The Pitot tube was installed on the left side of the fuselage. In addition, the 3D printed five-hole probe is situated on the nose of the drone, the holes being connected to three differential pressure transducers (HCEM010, sampled at 100 Hz) by silicone tubes (Fig. 3). It has five pressure ports; the center hole is in the longitudinal axis of the airplane, and permits to measure the stagnation pressure and to calculate the airspeed. The differential pressure between the up and down (resp. left and right) holes is used to calculate the angle of attack α (resp. angle of sideslip β).

Finally, the navigation of OVLI-TA is assured by 3DR Pixhawk autopilot which also contains a GPS and an IMU, the data are recorded at 5 and 50 Hz, respectively. The overall equipment is presented in Fig. 4.

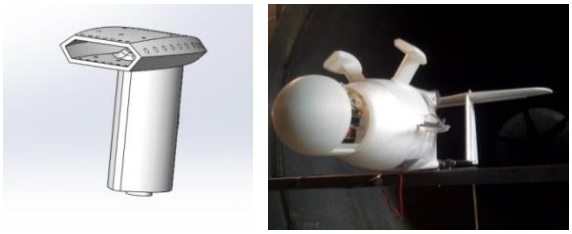

Figure 2: Illustration of the hoods where the temperature and humidity sensors are placed

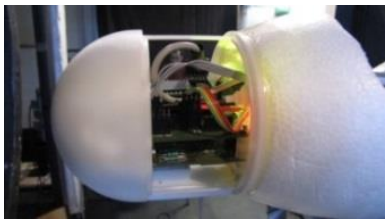

Figure 3: The 5-hole probe situated in the nose of the UAV

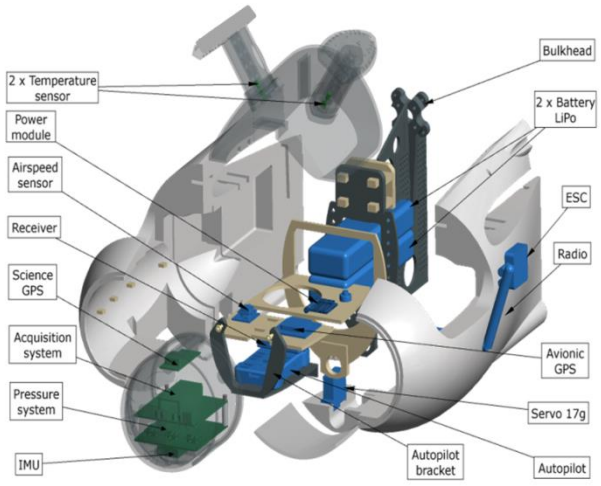

Figure 4: Exploded diagram of electronic devices on OVLI-TA

2.3. Characteristics of "BOREAL":

The airplane utilized is a Boreal-UAS, from BOREAL- groupe MISTRAL company (Fig. 5).

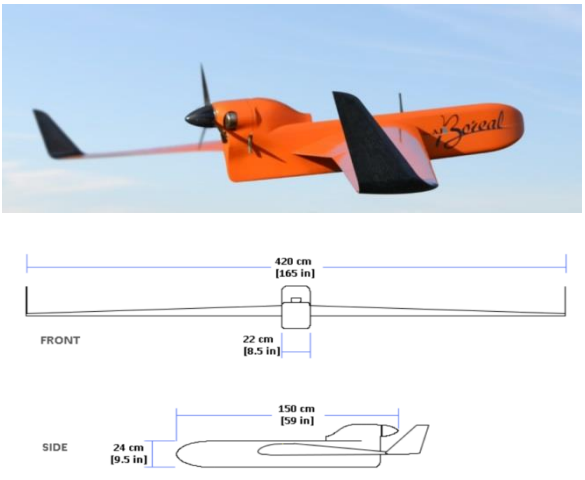

Figure 5: Pictures of BOREAL UAV

Boreal is powered by a combustion engine and the cruise speed varies between 70 km/h and 130 km/h (19-36 m/s). The wingspan is 4.2 m and the fuselage length is 1.50 m. This UAV weighs 20 kg and can embark 5 kg of payload. The best advantage of Boreal is its high endurance that can attain 10 hours of flight.

2.4. Electronic devices on BOREAL:

The BOREAL is outfitted with a 100 Hz μSD card, and two temperature and humidity sensors SHT75 (a slow one at 2.5 Hz and a faster one at 10 Hz), in addition to a fast temperature sensor (PT1000) at 100 Hz, all three are placed inside the hoods (Fig. 2).

We choose to embark the Air Data Unit Advanced Navigation (25Hz), which provides us with pitch, yaw and roll measurements, and also ground speed, wind speed, airspeed, barometric pressure, and accelerations. The miniature GPS inside it that is aided with inertial navigation system and AHRS (Altitude and Heading Reference System), provides accurate positioning.

The 3D printed five-hole probe situated in the nose of the UAV is connected to the digital pressure sensors through silicone tubes (Fig. 6). We have chosen transducers with a different principal of measurements than those used for OVLI-TA, in order to reduce the impact of drone vibrations on the turbulence measurements.

One Pitot tube and static ports are also implemented. The Boreal is navigated using Boreal's autopilot.

Figure 6: Picture of the five-hole probe on BOREAL

3. Wind tunnel calibrations of the five-hole probe:

3.1. For OVLI-TA:

The wind tunnel test is necessary in order to calibrate the five-hole probe of OVLI-TA. It was conducted in the IMFT (Institut de Mécanique des Fluides de Toulouse) wind tunnel in 2014.

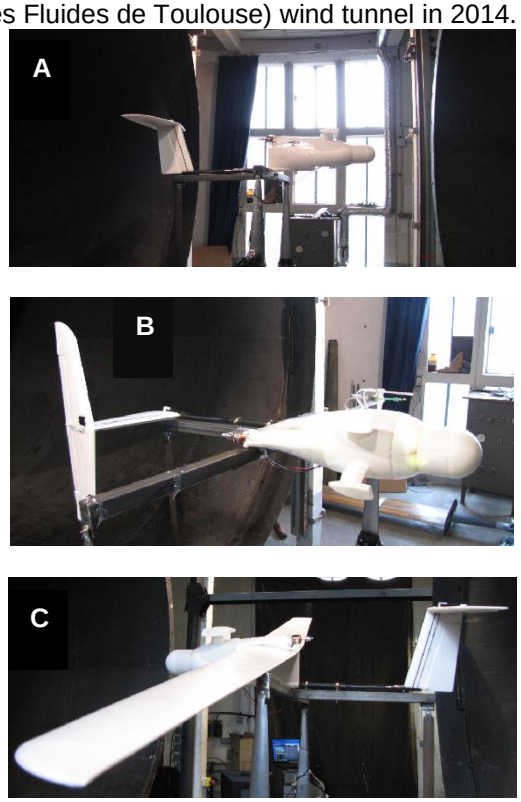

Figure 7: OVLI-TA during the wind tunnel test: A) Angle of attack testing; B) Angle of sideslip testing; C) Roll testing with wing mounted. [16]

The data acquisition system was installed as during the flights. Figure 7 shows how the UAV is installed in the wind tunnel.

The sensitivity factor is defined as:

$$\alpha = k_{\alpha}^{-1} * \widehat{\Delta P_{\alpha}} \quad (1)$$

$$\beta = {k_{\beta}}^{-1} * \widehat{\Delta P_{\beta}} \quad (2)$$

The angle of attack was varied between -5° and 5° with a zero angle of sideslip, so as to determine the sensitivity factor k_{α}. The relationship between the differential normalized pressure and IMU's angle of attack is shown in Fig. 8.

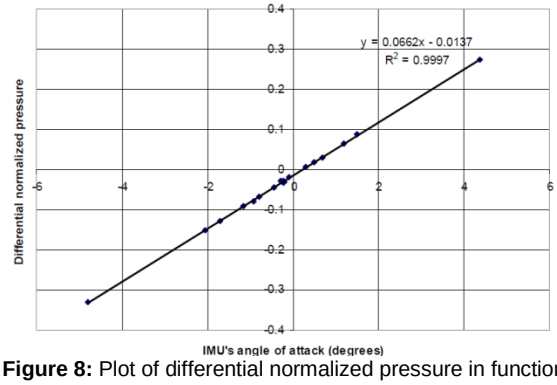

Figure 8: Plot of differential normalized pressure in function of angle of attack [16]

From this plot we can deduce that the sensitivity factor of the attack angle is:

$$k_{\alpha} = 0{,}0662 \text{ deg}^{-1}$$

In the same way, the angle of sideslip was varied between -5° and 5° by maintaining the angle of attack equal to zero, in order to determine the sensitivity factor k_{β}. The relationship between the differential normalized pressure and IMU's angle of sideslip is shown in Fig. 9.

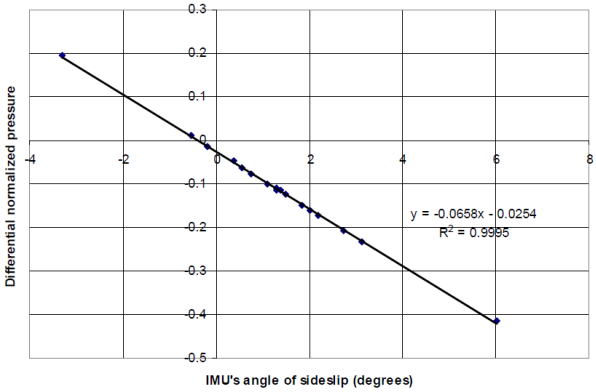

Figure 9: Plot of differential normalized pressure in function of angle of sideslip [16]

According to the Fig. 9, the sensitivity factor of the sideslip angle is: $k_{\beta} = 0{,}0658 \text{ deg}^{-1}$.

By using formulas 1 and 2 and the sensitivity factor found after wind tunnel calibration, we can calculate the angles of attack and sideslip during the flights.

3.2. For BOREAL:

The calibrations of the five-hole probe of Boreal UAV, was also done in the IMFT wind tunnel in 2017 [7].

The data acquisition system was installed as during the flights. The setup of the wind tunnel test is illustrated in Fig. 10.

Figure 10: BOREAL during the wind tunnel test

The angles of attack and sideslip were varied between -15° and 15° with respectively a zero angle of sideslip and a zero angle of attack. The relationship between the differential normalized

pressure and IMU pitch is shown in Fig. 11.

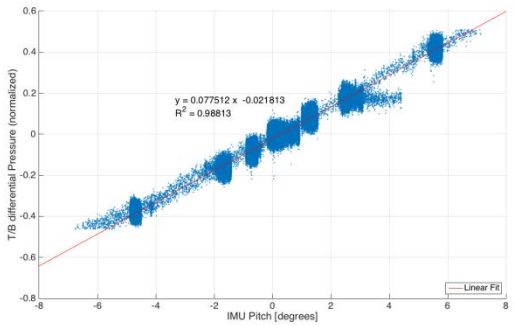

Figure 11: Plot of differential normalized pressure in function of angle of attack (reprinted from [7]).

So, the sensitivity factor for the attack angle is: $k_\alpha = 0{,}0775 \ \ \mathrm{deg}^{-1}$. This value is near to the value obtained in theory [5] which is equal to 0,078 deg^{-1}.

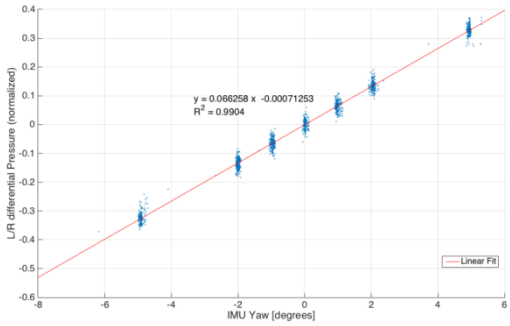

Figure 12: Plot of differential normalized pressure in function of angle of sideslip (reprinted from [7])

According to Fig. 12, the relationship between the differential normalized pressure and IMU's yaw implies that the sensitivity factor for the angle of sideslip is: $k_\beta = 0{,}0663 \ \mathrm{deg}^{-1}$. Note that the sideslip data was taken every 3 seconds only due to a recording issue during the wind tunnel test.

4. Field results and discussion:

OVLI-TA flew in two different sites. Firstly, the flight tests were conducted in Lannemezan, France. Then the drone participated in DACCIWA campaign in West Africa (Savé, Bénin).

4.1. Results of flight test on Lannemezan site:

Lannemezan site is the instrumental site of the "Laboratoire d'aérologie". It is equipped with an instrumented mast of 60 m (see Fig. 13).The mast is equipped at three levels (30 m, 45 m, 60 m) for turbulence measurements with sonic anemometers that give us the 3 wind components and the so-called sonic temperature at a frequency of 10 Hz. In addition to that, relative humidity and temperature are measured at those levels and recorded at 1 Hz.

Figure 13: *Picture of the instrumented mast of 60 m at Lannemezan Site*

The flight pattern chosen is a succession of straight and level paths that is the most appropriate type of flight plan for atmospheric turbulence measurements (Fig. 14).

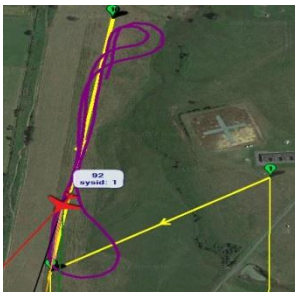

Figure 14: Flight with straight lines

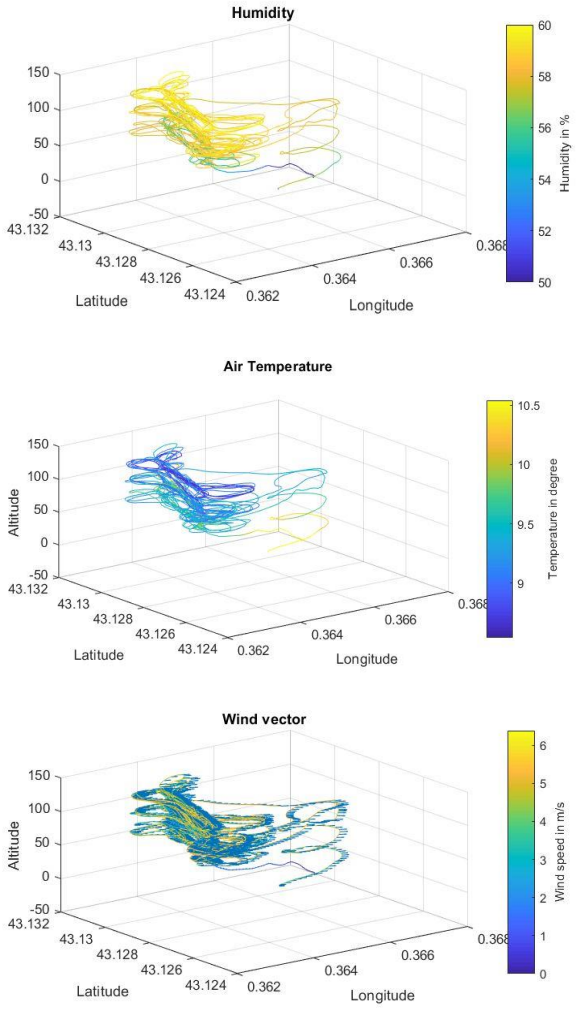

Figure 15: Humidity, temperature and wind speed measured by OVLI-TA

Figure 15 shows the measurements done by OVLI-TA during approximately one hour of flight in Lannemezan.

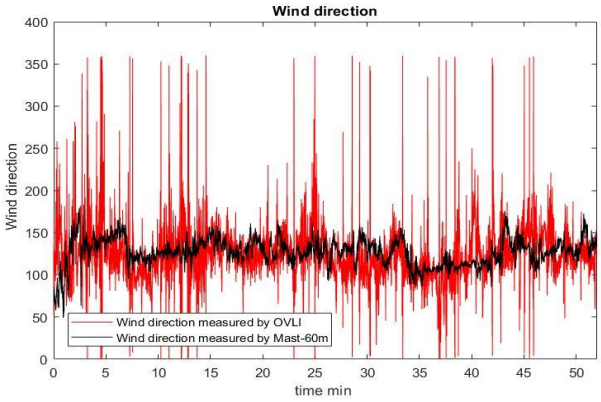

Figure 16: Wind speed and wind direction measured by OVLI-TA and on the mast at 60m.

Figure 16 compares the wind speed and wind direction measured by OVLI-TA (curve in red) to those measured by the mast at 60 m level. We can see that the two measurements are coherent, though the OVLI-TA signal presents a higher variability, at least in part related to poorer wind estimates during half turns between two straight flights.

During the 1 hour flight, we selected 61 sequences of straight line flights at almost constant altitude; each of them lasting around 30 s. The height of these sequences was between 60 and 130 m agl. Figure 17 presents for one sequence the energy spectra of the north (VN), east (VE) and vertical (W) wind components.

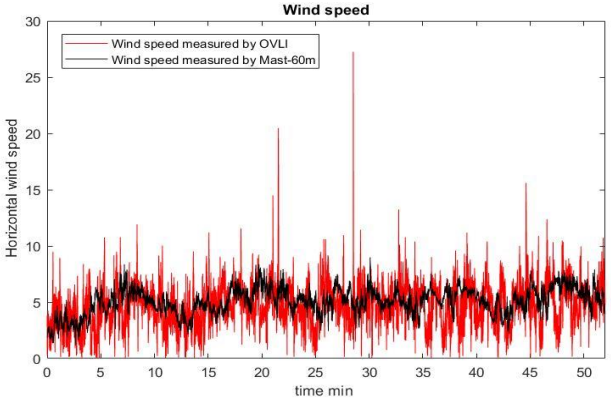

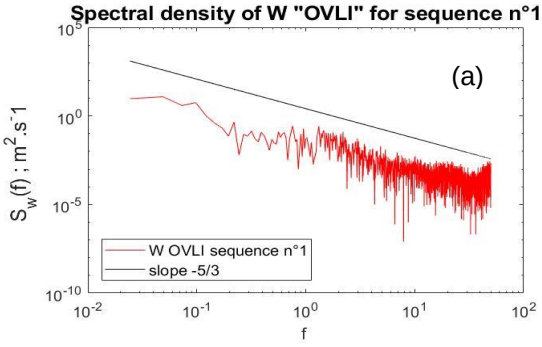

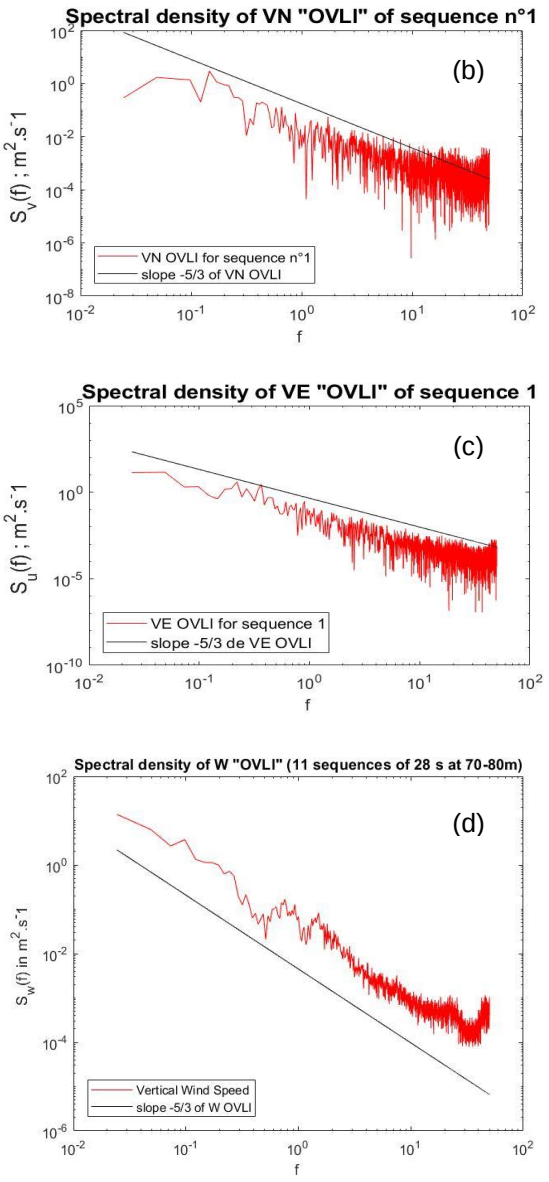

Figure 17: (a) Spectra of vertical wind speed, (b) north wind speed, (c) east wind speed. (d) Mean spectrum of vertical wind speed of 11 sequences of straight and level flight at 70-80m agl.

Moreover, the mean spectrum of vertical wind speed computed over 11 sequences of identical duration and performed at comparable height (70-80m) is presented in Fig. 17 (d). The -5/3 slope, characteristic of the inertial subrange, is observed on these spectra up to a frequency of around 10 Hz.

In order to compare between mast and drone spectra, we should go back to the same scale by converting the frequencies *f* into wavenumbers *k*, considering a speed *u* which is the mean airspeed for OVLI and the mean wind speed for the mast (in other words, assuming Taylor hypothesis: $k=2\pi f/u$.) This comparison, presented in Fig. 18 for the vertical wind speed on the 1st sequence of straight flight, shows a good correspondence between the two platforms up to wavenumbers of ~4-5 rad/m.

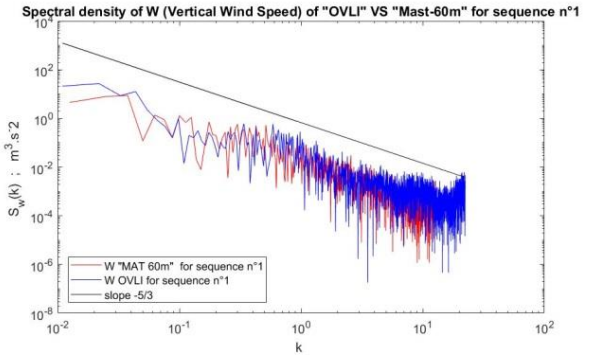

Figure 18: Vertical wind spectrum as a function of the wavenumber, computed on the 1st straight sequence of the drone OLI-TA (in blue) and on the 60 m mast (in red).

4.2. DACCIWA site

OVLIT-TA participated in the international project DACCIWA (Dynamics-Aerosol-Chemistry-Clouds Interactions In West Africa), in Savè, Bénin. The ground-based field campaign took place during June and July 2016.

Figure 19: DACCIWA SITE, in Savè, Bénin

The site was equipped with radio soundings, remotely piloted airplane system, cloud camera, cloud radars, Doppler lidars, UHF wind profiler and meteorological/turbulence/chemistry ground stations (Fig. 19).

The OVLI flight pattern consisted of straight and level runs of similar lengths as shown in Fig. 20. The drone flew between 10 m and 1000 m agl, with ascending circles and descending straight lines.

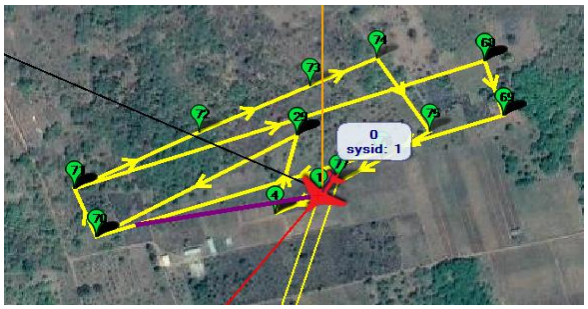

Figure 20: Flight with straight lines and loiter

Figure 21 shows the wind vector and temperature measured by OVLI during the flight of 15/07/2016. The drone gives good global measurements; in particular the wind vector was consistent whatever the heading of the airplane.

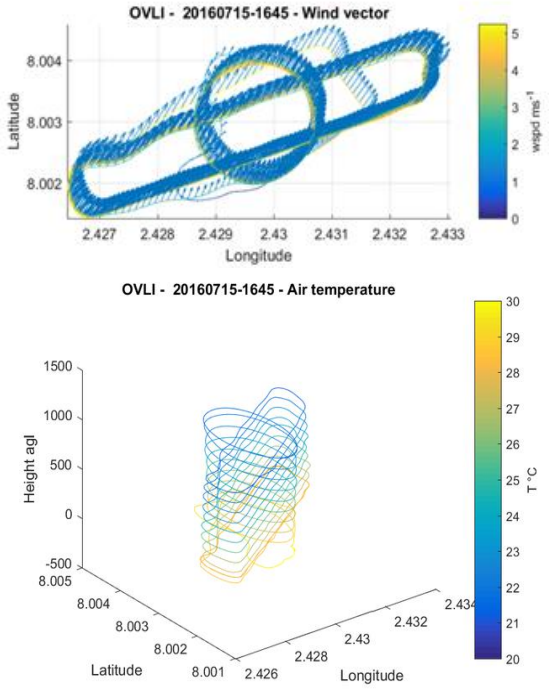

Figure 21: Wind vector and air temperature measured by OVLI

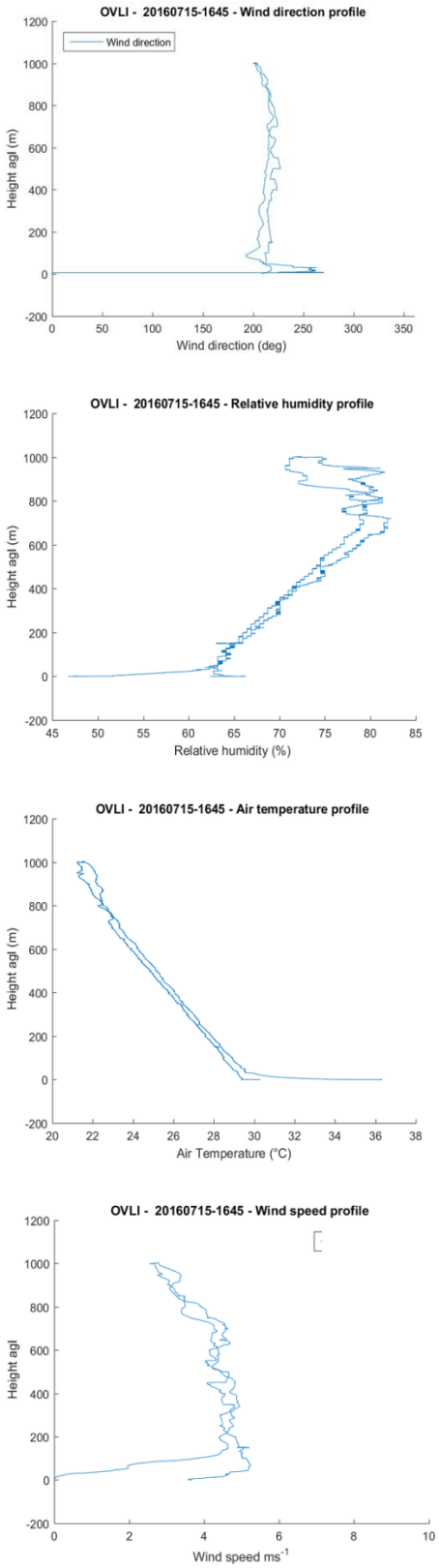

Figure 22: Altitude respectively in function of Wind direction, relative humidity, temperature and wind speed throughout the flight in July 15

Another check of the quality of the measures is to compare profiles during ascending and descending parts of the flight. This is shown in Fig. 22, for the wind speed and direction, relative humidity and temperature. The consistence between the two sequences is satisfactory.

5. Conclusion

OVLI-TA UAV is capable of measuring the temperature, humidity and three wind components. The raw data during the flight test were compared to 60 m mast measurements; the spectra show a good agreement between fixed and mobile platforms even if we were not exactly flying in the footprint of the mast. OVLI-TA was deployed during the DACCIWA campaign, where it performed atmospheric profiles between ground level and 1000 m. Recently, the development of new instrumentation on Boreal drone enhances the observation capabilities over long distance / long duration. Furthermore, a heavier instrumental package allows us to embark high-performance instruments, in particular for turbulence measurements. Flight tests have already been conducted, flight calibrations are planned on the Lannemezan site in the coming months, and next year we would be able to participate to field campaigns.

Acknowledgements:

The DACCIWA project has received funding from the European Union Seventh Framework Programme (FP7/2007-2013) under grant agreement no. 603502. OVLI-TA development was supported by CNRS-INSU LEFE program and Observatoire Midi-Pyrénées. The instrumental package onboard the Boreal is made possible thanks to the support of the European Union and the Région Occitanie through the MIRIAD program, and of the RTRA STAE foundation through the EG2R program.

References:

[1] Kaimal, J. C., and Finnigan, J. J. Atmospheric boundary layers flows: Their structure and measurement. Oxford: Oxford university press, 1994.

[2] Lenschow, Donald. H. Aircraft Measurements in the boundary Layer, In, Probing the Atmospheric Boundary Layer, Lenschow, Donald. H, p 39-55. Boston: American Meteorological society, 1986.

[3] Stull, Roland. B. An introduction to boundary layer meteorology. The Netherland: Kluwer Academic Publishes, 1988.

[4] Brown, E. N., Friehe, C.A., and Lenschow,D. H. The use of pressure fluctuations on the nose of an aircraft for measuring air motion. Research Aviation Facility, National Center For Atmospheric Research, Boulder. Journal of climate and applied meteorology 171-180, 1982.

[5] Rhudy,M., Larrabee,T., Chao,H., Gu,Y., and Napolitano, M.R. UAV attitude, heading, and wind estimation using GPS/INS and an air data system. American Institute of Aeronautics and Astronautics (AIAA), 2013.

[6] Elston, J., Argrow, B., Stachura, M., Weibel, D., Lawrence, D., and Pope, D. Overview of small fixed-wing unmanned aircraft for meteorological sampling. J. Atmos. Ocean. Tech., 32, 97-115, 2015.

[7] Gomez Kuri, Z. Atmospheric turbulence study utilizing a five-hole probe on an unmanned aerial vehicle (UAV), Master thesis, 2017.

[8] Barton, Jeffrey D. Fundamentals of Small Unmanned Aircraft Flight. Johns Hopkins Apl Technical Digest, 31(2), 132-149, 2012.

[9] Bonin, T. A., Chilson, P. B., Zielke, B. S., Klein, P. M., and Leeman, J. R. Comparison and application of wind retrieval algorithms for small unmanned aerial systems. Geosci. Instrum. Method. Data Syst., 2, 177–187, 2013

[10] Premerlani, W. IMU wind estimation (theory). 2009.

[11] Bonin, T. A., Zielke, B., Bocangel, W., Shalamunenc, W., and Chilson, P. B. An analysis of wind retrieval algorithms for small unmanned aerial systems. American Meteorological Society conference. (10.3).

[12] Khelif, D., Burns, S. P., and Friehe, C. A. Improved Wind Measurements on Research Aircraft. Department of Mechanical and Aerospace Engineering, University of California, Irvine, California. J. Atmos. Ocean. Tech., 16, 860-875, 1998.

[13] Taylor, G.I. The Spectrum of Turbulence. The royal society publishing. 476-490, 1937.

[14] Wildmann, N., Ravi, S., and Bange, J. Towards higher accuracy and better frequency response with standard multi-hole probes in turbulence measurement with remotely piloted aircraft (RPA). Germany. Atmos. Meas. Tech., 7, 1027–1041, 2014

[15] Willis, G.E. and Deardorff, J.W., 1976. On the use of Taylor's translation hypothesis for diffusion in the mixed layer. Quart. J. Roy. Meteor. Soc., 102, 817-822.

[16] Cernov, I. Study of the atmospheric turbulence measurement by a probe on a light drone, Master thesis, 2014.